SIEMENS

White Paper

Tissue Strain Analytics

A Complete Ultrasound Solution for Elastography

John Benson BS, RDMS, RDCS
Director, Clinical Applications

Liexiang Fan, Ph.D.
Senior Key Expert

Answers for life.

White Paper

Tissue Strain Analytics – A Complete Ultrasound Solution for Elastography

John Benson BS, RDMS, RDCS
Director, Clinical Applications

Liexiang Fan, Ph.D.
Senior Key Expert

Introduction

Ultrasound imaging is a first-line imaging modality for a wide range of indications, playing a major role in screening, diagnosis and therapeutic interventions for various diseases and pathologies. Continuous improvement in conventional ultrasound technology, including real-time B-mode, Doppler and color flow imaging has provided exquisite visualization of anatomy and physiology with high spatial and contrast resolution, particularly in superficial structures such as breast, thyroid, musculoskeletal structures and the cardiovascular system. However, conventional ultrasound is limited in its ability to differentiate between the mechanical properties of tissue, which can be important in assessing the morphology and physiology of focal or diffuse disease.

Tissue strain analytics provide a new dimension in ultrasound imaging, enabling both qualitative and quantitative assessment of the mechanical stiffness (elasticity) differences in tissue. Siemens, the pioneer in ultrasound elastography, provides the most comprehensive “toolbox” of complementary tissue strain analytic applications in the ultrasound industry today. Siemens’ ACUSON S Family™ ultrasound systems can be configured with a wide range of tissue strain analytic technologies and applications, helping physicians to solve their most difficult diagnostic problems.

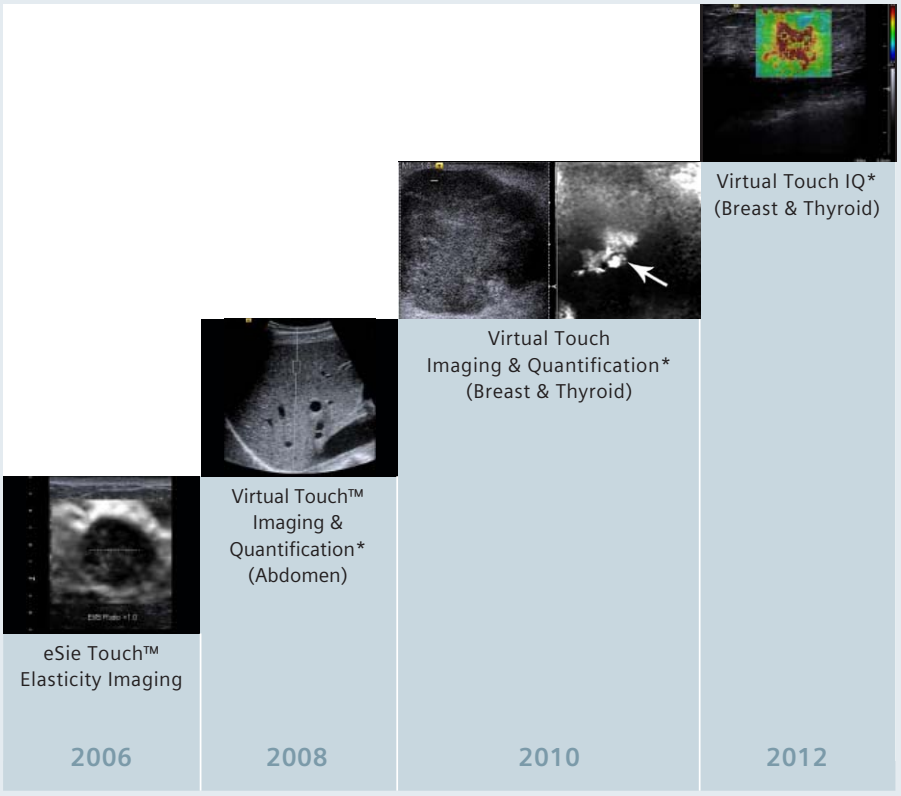

Figure 1: Evolution of Siemens' Tissue Strain Analytics Applications.

*Not commercially available in the USA.

Complementary Tissue Strain Technologies

As the saying goes, in order to get the best results you need to use the right tool. This is certainly true in tissue strain analytics. The perfect diagnostic tool would have 100% sensitivity (a positive result when disease is present) and 100% specificity (a negative result in the absence of disease) in all cases. Such a technology does not exist in diagnostic imaging, however, the use of more than one imaging tool can provide overall higher diagnostic accuracy than one imaging modality alone. Siemens' ACUSON™ ultrasound systems are unique in this regard, as they provide multiple technological solutions that are each optimized for specific applications and clinical problems. The end result is an overall higher sensitivity and specificity in different disease states compared to conventional ultrasound alone, or even a single form of elastography.

Core tissue strain imaging performance is enabled by the unique signal processing architecture of Siemens' ACUSON S Family ultrasound systems. Extremely small changes in tissue displacement (in the order of 1–10 microns) are tracked and computed using the RF acoustic signal and sophisticated algorithms. The ability to detect such small tissue displacements results in highly sensitive and reproducible diagnostic images.

eSie Touch™ elasticity imaging's name is derived from its ability to obtain a high contrast-to-noise ratio, and high resolution elastograms with minimal requirement for tissue compression by the transducer surface. Although the underlying stress forces required for tissue strain analysis employ simple manual compression techniques, native tissue motion alone, induced by the patient's cardiac pulsations and respiration, is typically sufficient for high quality image acquisition. eSie Touch elasticity

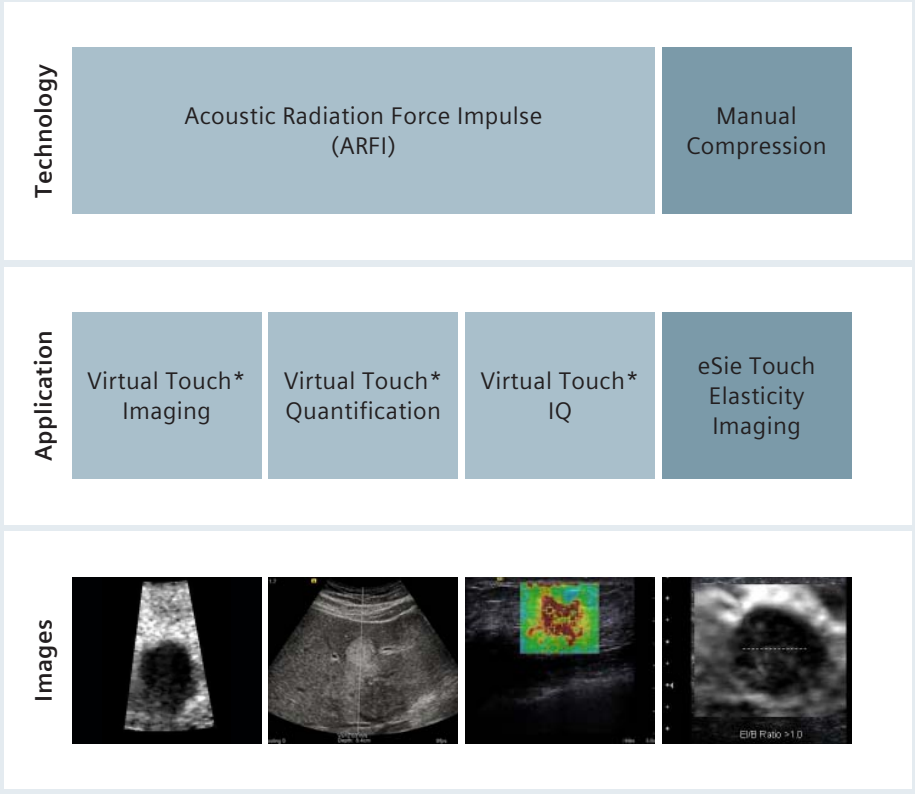

Figure 2: Siemens' Tissue Strain Technologies and Applications.

*Not commercially available in the USA.

imaging is available on all ACUSON S Family – compatible Siemens' curved linear array and linear array transducers, as well as an endocavity transducer, providing real-time assessment of relative tissue strain (stiffness) in breast, thyroid, musculoskeletal and abdominal applications.

Virtual Touch™* is a family of applications founded on the principle of acoustic radiation force impulse (ARFI) technology. Rather than relying on manual compression techniques, tissue is compressed using an acoustic push beam. One advantage of Virtual Touch technology is that the push beam is focused at the region of interest (ROI) to maximize the local displacement of tissue via the acoustic impulse, rather than just at the skin surface with uncontrollable stress being applied in deeper tissues. The ability to focus the push beam results in a more controllable application of stress, therefore, uniformity of the resulting elastogram is improved. Another advantage is the ability to induce and track the propagation of shear (transverse) waves for quantification of tissue stiffness. An increase in shear wave velocity correlates closely with increasing tissue stiffness, providing a more precise indication of true tissue elasticity. A third, but important advantage, is the reduction in user technique dependence. The user simply initiates the acquisition of the elastogram or quantitative measurement with the push of a button, further improving inter-operator reproducibility, which is an important aspect of clinical utility.

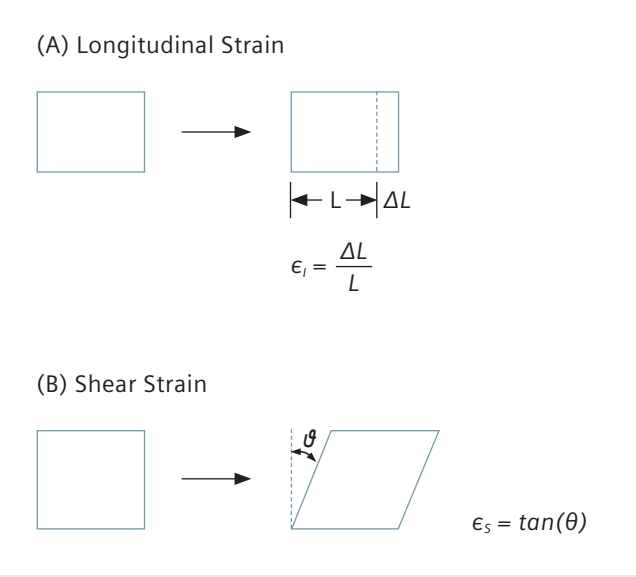

Figure 3: (A) Longitudinal and (B) Shear Strain.

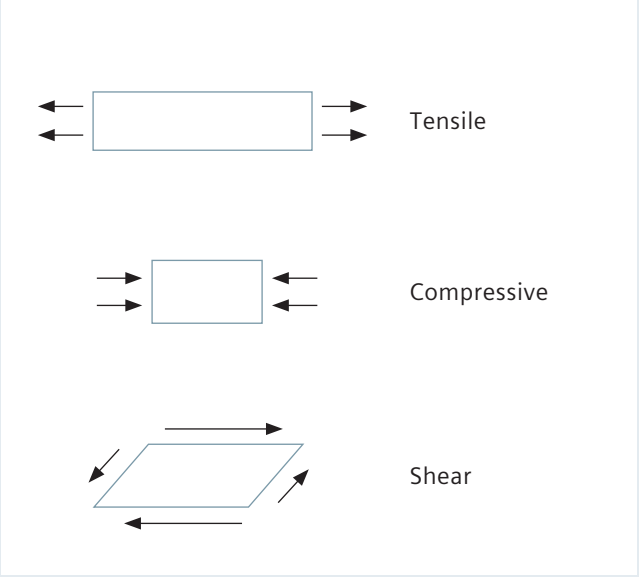

Figure 4: Stress and Strain.

Mechanical Properties of Tissue

It is well known that soft tissue is elastic. Many studies have been performed to characterize the normal range of elasticity values of various tissue types [1, 2], and that certain disease processes can change the viscoelastic properties of tissue. Therefore, tissue elasticity imaging provides an independent dimension of information in clinical application.

The concept of strain can be understood by examining the local change in length of a small volume of tissue. Two kinds of strain exist, as illustrated in Figure 3.

Longitudinal, or normal strain, occurs when tissue is either stretched or compressed. Shear strain occurs as a result of angular forces, such as twisting or bending.

In tissue, both longitudinal and shear strains are usually present when manual compression force or radiation force is used. Poisson's Ratio for a given tissue type provides us with a ratio of transverse strain to the normal longitudinal strain. The concept of stress in tissue is illustrated in Figure 4.

In fluid, pressure is the same in all directions, therefore, shear strain and shear waves do not exist in fluids. The tensile character of stress at a point, however, is quite complex and rather unusual combinations of tensile, compressive and shear components exist on each face of a three dimensional cubic element.

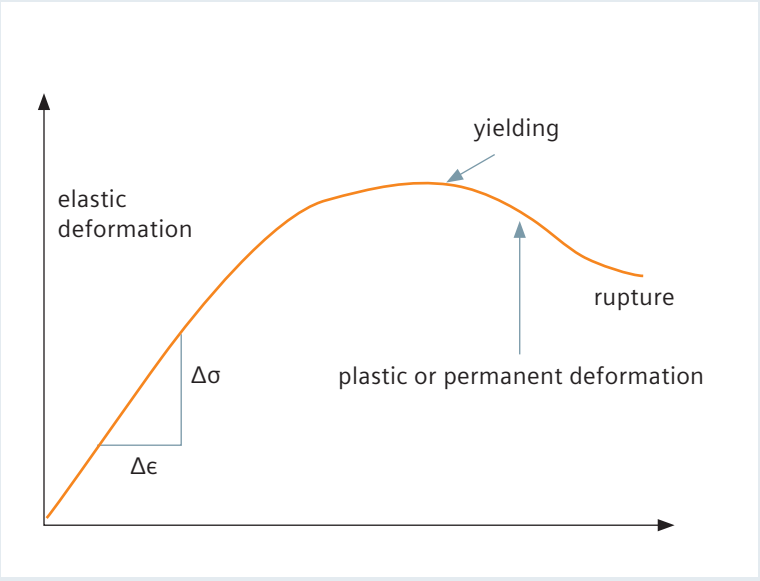

Figure 5: Relationship between Stress and Strain in Material.

Hooke's law, or $\sigma = Y\epsilon$, gives us a relationship between stress and strain for most materials, including viscoelastic tissue. *Y* is called the Young's Modulus or Modulus of Elasticity and can be computed by examining the slope of the stress/strain diagram in the elastic portion of the curve, as shown in Figure 5.

The shear modulus *G*, also known as the Modulus of Rigidity, can be calculated in a similar fashion from a corresponding shear stress vs. shear strain curve.

In homogeneous and isotropic tissue, there are two kinds of waves, pressure (longitudinal compression) waves and transverse (shear) waves. In elastic materials, the relationship between the velocity of a shear wave (v_s), and shear modulus is,

$$v_s = \sqrt{\frac{G}{\rho}}$$

where G is the tissue shear modulus
ρ is the solid tissue density

Tissues with a higher shear modulus, or modulus of rigidity (less compliant to shear forces) will have a higher shear wave velocity than tissues with a lower modulus of rigidity (more compliant to shear forces).

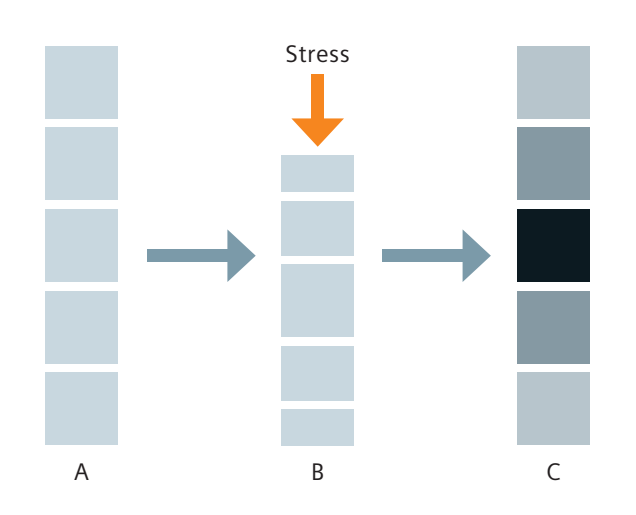

Figure 6: Adjacent tissue elements may appear identical (isoechoic) using conventional B-mode or Doppler imaging (A). However, when a stress (longitudinal force) is applied to these tissues, they may behave differently with some experiencing greater deformation than others (B). By comparing the baseline and deformed information, individual tissue elements may be labeled by their relative stiffness. A light shade indicates relative soft (elastic) tissue, while a darker shade indicates relative stiffness (non-elastic) tissue (C).

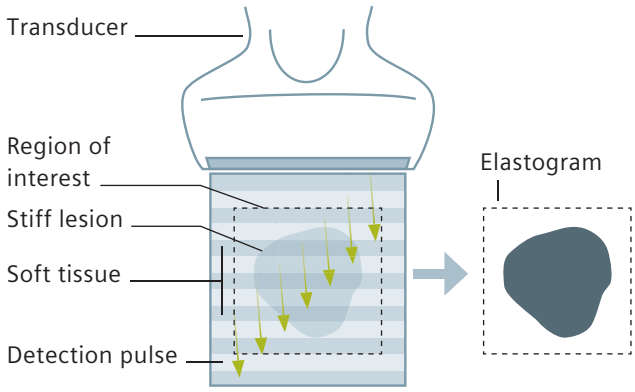

Figure 7: Tissue strain is induced by minimal **mechanical compression** with the transducer or cardiac pulsations and respiration. Detection pulses track displacement, which are used to derive a strain image in gray scale or color-coded display.

Technology Overview

eSie Touch Elasticity Imaging

With eSie Touch elasticity imaging, the elastogram is created using either minimal compression or physiologic tissue motion from cardiac pulsations, or respiration as the stress force on tissue. Compressive strain of tissue is recorded in the image through continuous analysis of acquired ultrasonic detection signals. Figure 6 illustrates how relative compressive differences are coded into the image using gray scale or color-coded elastogram maps.

Figure 7 illustrates the relationship of detection beams within the image and the user defined region of interest.

Virtual Touch* Imaging

A Virtual Touch image is a grayscale or color-coded display of relative tissue stiffness in a user-defined region of interest. This information is computed by examining the displacements of tissue elements in response to an acoustic push pulse. Detection and computation of relative elasticity is similar to eSie Touch elasticity imaging. Virtual Touch imaging forms an image by combining independently acquired multiple lines of tissue displacement information as shown in Figure 8.

In contrast to conventional ultrasound imaging pulsing strategy, Virtual Touch imaging uses a three-step pulsing method. First, a conventional ultrasound signal is acquired as a baseline in a narrow region of interest.

*Not commercially available in the USA.

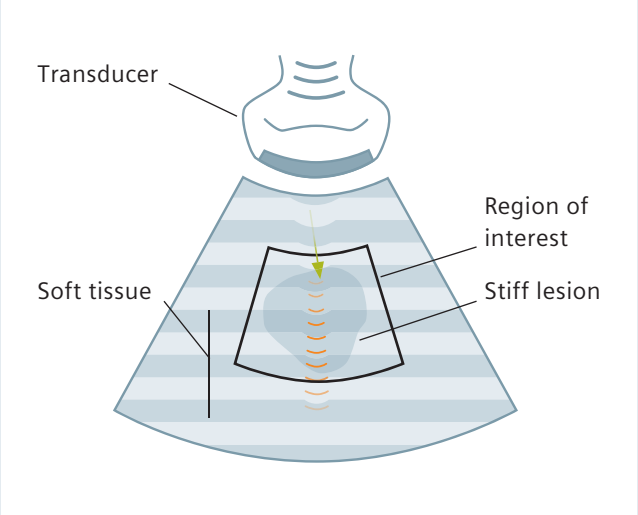

Figure 8: Virtual Touch imaging utilizes acoustic push pulses (orange) and detection echo (green arrow), sequenced across a user-defined region of interest, to generate a displacement map depicting the relative stiffness of tissue.

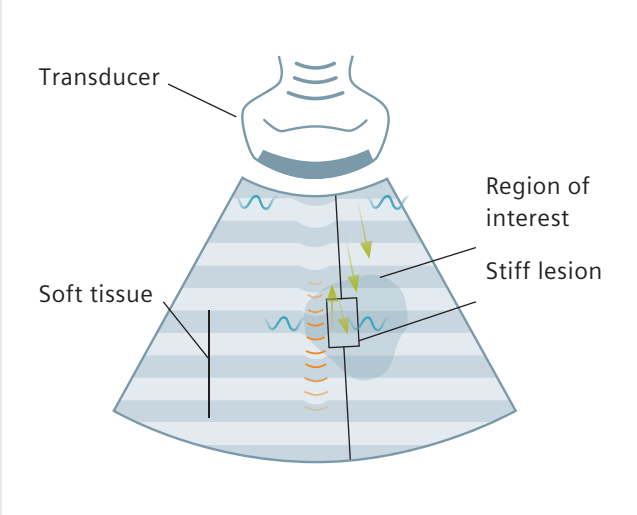

Figure 9: Virtual Touch quantification utilizes an acoustic push pulse (orange) to generate shear waves (blue) through a user-defined region of interest. Detection pulses are applied in multiple locations and reveal arrival time, allowing calculation of the shear wave propagation speed.

Second, a push pulse is applied along the center of this region of interest. Third, another conventional ultrasound signal is acquired and is compared to the baseline to obtain tissue displacement. The more elastic a given tissue element, the more displacement it experiences. This process is repeated for each axial line within the region of interest, as with a conventional B-mode image.

Virtual Touch Quantification

In addition to displacing the tissue residing within the acoustic push pulse path, shear waves are generated after the application of the focused push pulse. These shear waves propagate perpendicular to the push pulse. In tissue, shear waves travel at a velocity of around 1–10 m/s, which is slow enough to be well sampled by detection beams. Shear waves are rapidly attenuated, with an attenuation coefficient significantly higher than that of longitudinal ultrasound waves. There is a close correlation between tissue elasticity and its associated shear wave velocity, as described in the section covering mechanical properties of tissue. By observing the shear wavefront arrival at multiple locations and correlating these locations with the arrival time, shear wave speed within the region of interest is estimated, as shown in Figure 9.

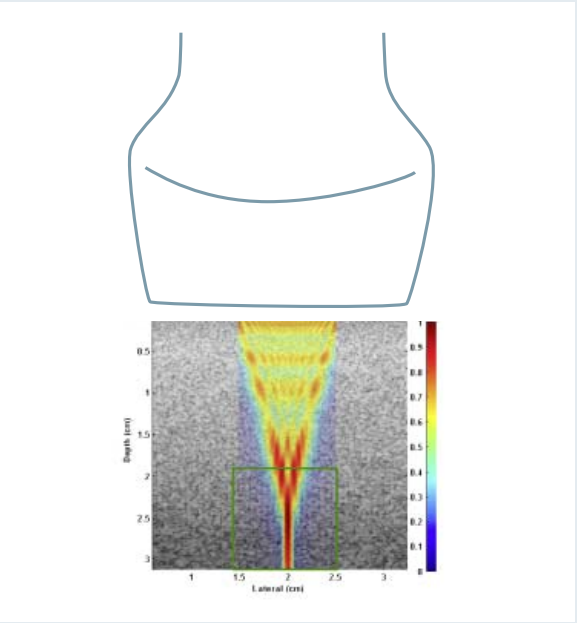

Figure 10: Illustration of focused ultrasound beam (color overlay in the echo image), region of interest (green rectangle box), and ultrasound transducer, which generates the focused beam and receives echo signal. The colors represent the relative acoustic intensity levels in the demonstrated beam, with the solid dark red color indicating the highest intensity level, while the light and transparent purple color represents lower intensity levels.

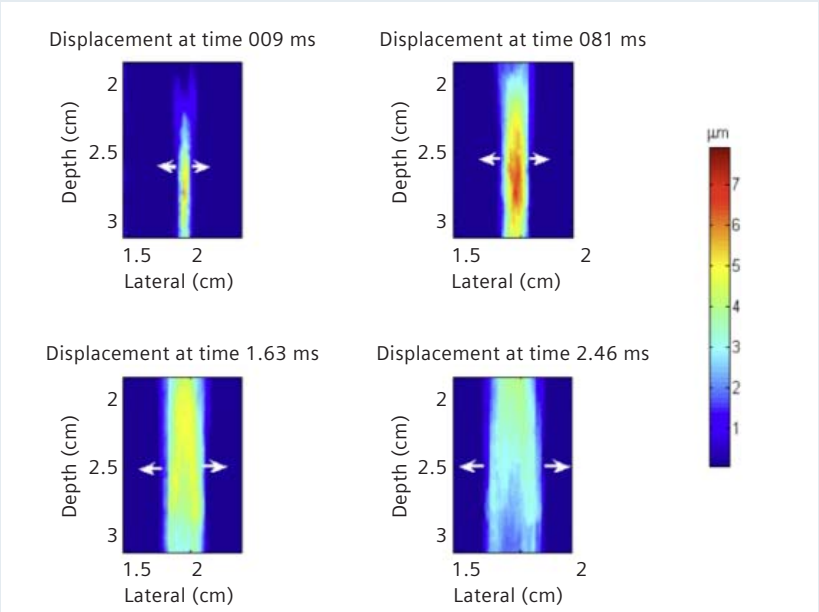

Figure 11: Illustration of tissue displacement information (both its spatial location and magnitude) after ARFI application. The four images show the displacement information at four observation times 0.09, 0.81, 1.63 and 2.63 milliseconds after the cessation of ARFI. The spatial scale in the four images are identical and the arrows in each image indicate that the spatial location of the displaced tissue moves outwards perpendicular to the ARFI beam application direction. The magnitude of tissue displacement decreases when distance from the ARFI beam increases, and the magnitude in the same spatial location changes over time.

Figure 10 illustrates the concept of creating shear waves within a region of interest using a focused push beam. Figure 11 demonstrates the propagation and attenuation of the displacement magnitude as the shear wave propagates out of the push pulse insonation location.

Virtual Touch IQ

Virtual Touch™ IQ provides the advantage of both quantitative and relative stiffness imaging combined in one display. The user defines a two-dimensional region of interest, which represents shear wave velocities at many point locations. The image is formed by a pulse sequence that is comprised of up to 256 acquisition beam lines. For each beam line, the system is instructed to sequentially acquire a noise level estimate, a number of reference vectors, application of ARFI excitation and then a relative large number of tracking vectors as shown in Figure 12. This sequencing takes place for one single location and gives the estimation of shear wave propagation time for each depth along the beam direction. By taking a similar data acquisition after moving the spatial location of the detection vectors to a location different than the first acquisition, a new line of shear velocity estimates is obtained. This line is in between the detection locations.

To generate an image of shear wave velocities, the above sequencing is repeated for all the lines in a region of interest as demonstrated in Figure 13. Although this demonstration shows the same number of beams in ARFI push pulses and detection vectors, when a parallel receiving beam is used in detection vectors, the beam number in ARFI pushing pulses can be reduced.

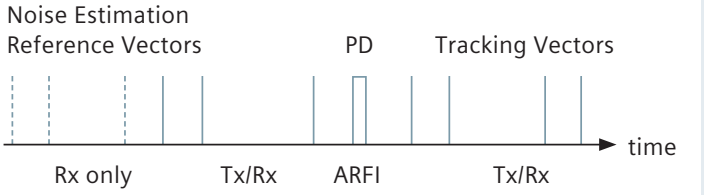

Figure 12: Data acquisition sequencing for a pair of ARFI excitation and detection locations. In the noise estimation segment there is no transmit (Tx), and the received echo signal (Rx) is used to estimate the noise level. In both reference vectors and tracking vectors, wide band transmit and receive is used to obtain the echo signals, and these signals are used to estimate the tissue displacement.

Courtesy of: Prof. Wu Chang Jun. Affiliated #1 Hospital of Harbin Medical University, China

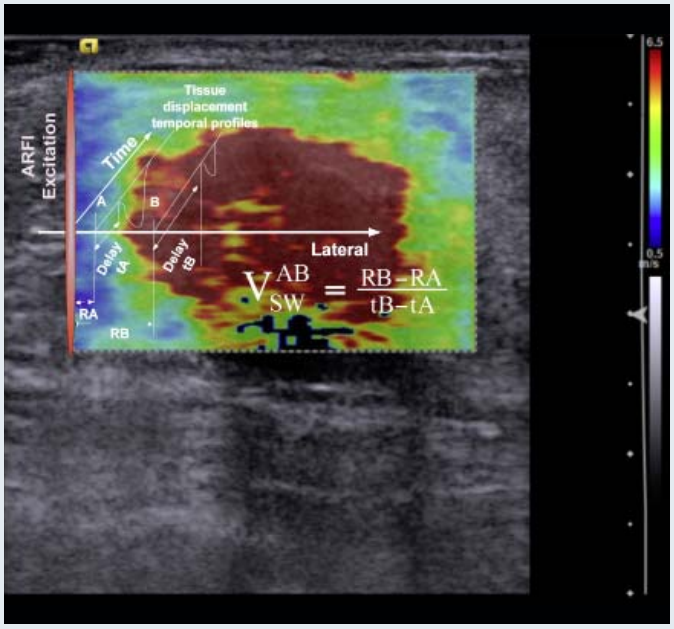

Figure 13: Illustration of ARFI excitation and shear wave represented by tissue displacement in spatial and temporal domain in Virtual Touch IQ scan mode. For each excitation, detection of shear waves take place at multiple lateral locations within a narrow lateral span, such as A and B shown in the figure. This excitation and detection sequence repeats by moving its lateral position in the VTIQ ROI to form up to 256 acquisition lines to provide high spatial resolution and high fidelity shear velocity estimate.

The distance between ARFI excitation and detection locations is set as constant when repeating the sequencing across the region of interest; therefore, estimating for shear velocity is a function of the travel time and the difference of travel times between detection locations.

Virtual Touch IQ (VTIQ) is capable of four discrete Shear Wave (SW) display modes:

1) Velocity
2) Quality
3) Travel Time
4) Displacement

These display modes assist the user in understanding the complex nature of shear waves that may confound image interpretation in the standard SW Velocity display.

The SW Quality display in particular is useful for interpreting whether the shear wave was of sufficient magnitude with adequate signal to noise (SNR) to accurately estimate shear wave velocity in the SW Velocity display. SW Displacement indicates the regions in tissue of low elasticity that may also be associated with higher SW velocity. The combination of these display modes provides additional information that when correlated create a better understanding of the shear wave displacement profile. Figures 14 and 15 demonstrate how shear waves behave in cystic structures and stiff solid lesions in tissue mimicking elasticity phantoms.

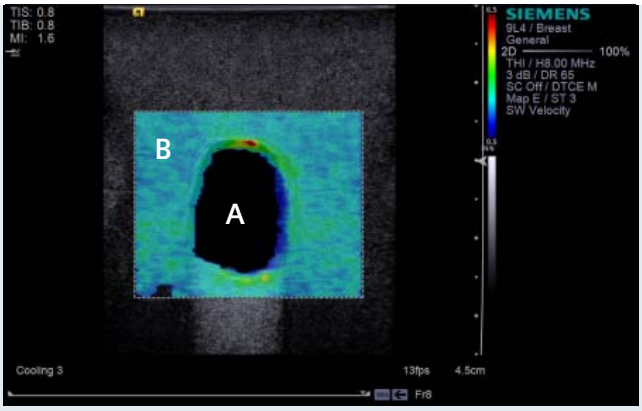

Shear Wave Velocity

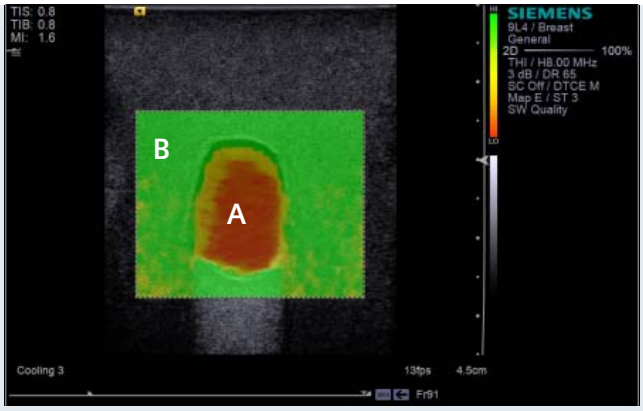

Shear Wave Quality

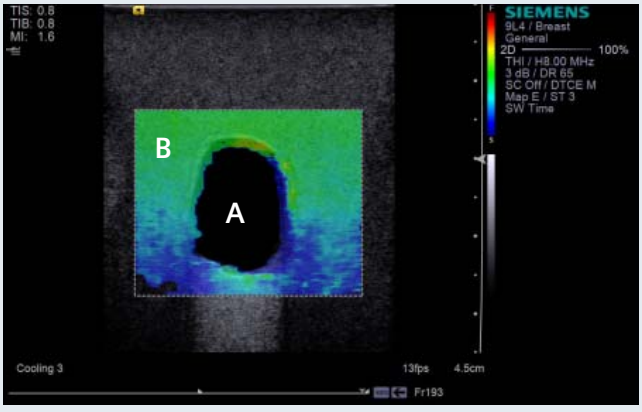

Shear Wave Travel Time

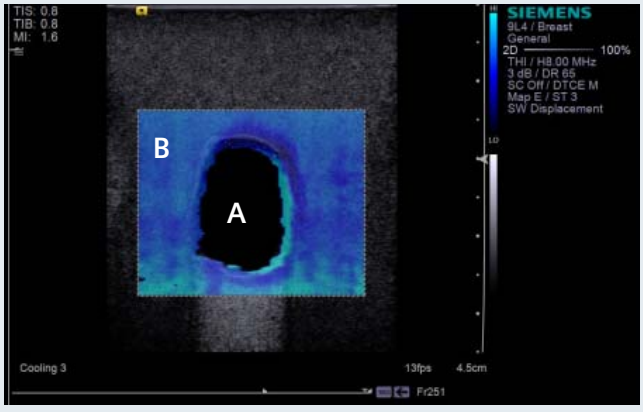

Shear Wave Displacement

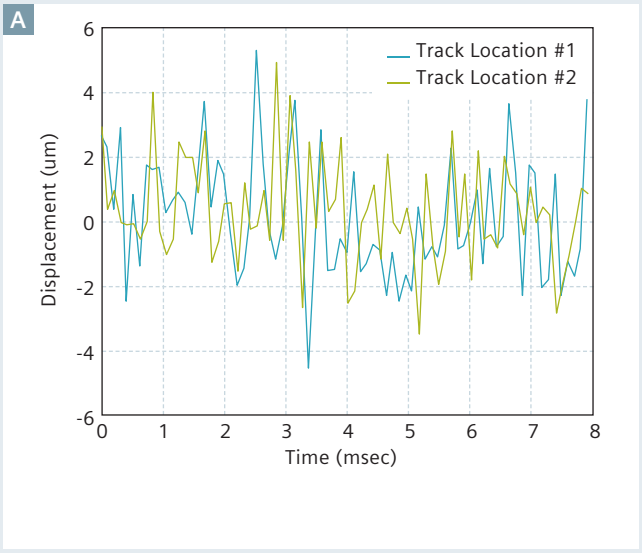

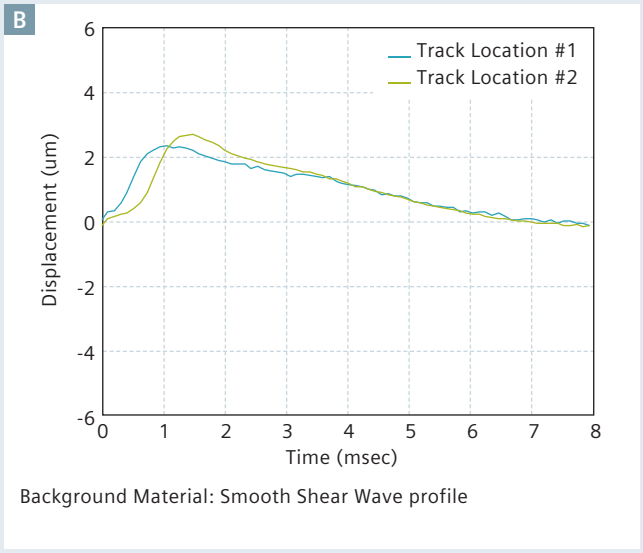

Background Material: Smooth Shear Wave profile

Figure 14: Tissue Mimicking Elasticity Phantom images with labeled regions: (A), a water filled simulated cyst and (B) solid background material. In the lower shear wave profiles as detected with RF acoustic data from paired detection beams, the cystic area in (A) is noisy without a distinct shear wave profile, consistent with fluid material that does not support shear waves. The smooth tissue displacement response of (B) indicates elastic material with the ability to detect a peak in each of the two displacement profiles at slightly different times and location, enabling shear wave velocity estimation. Note the low quality shear wave signal area representing the cystic area in red in the SW Quality display in the upper right image. The background material provides a high quality signal as indicated by the green area in the SW Quality display in the same image.

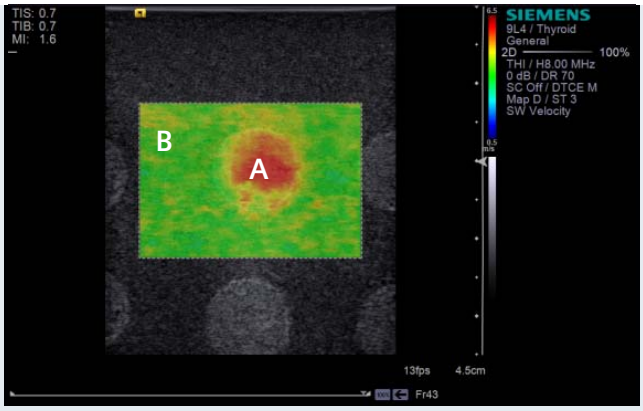

Shear Wave Velocity

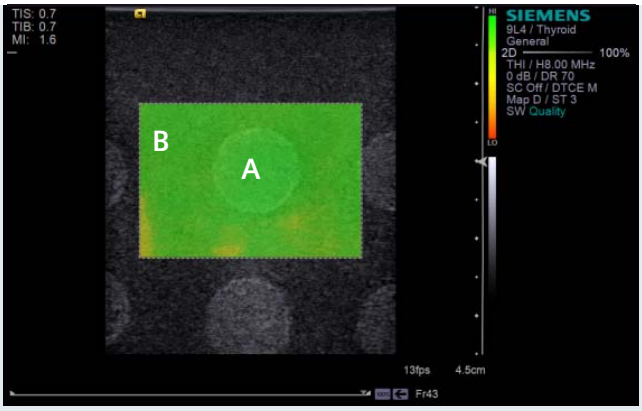

Shear Wave Quality

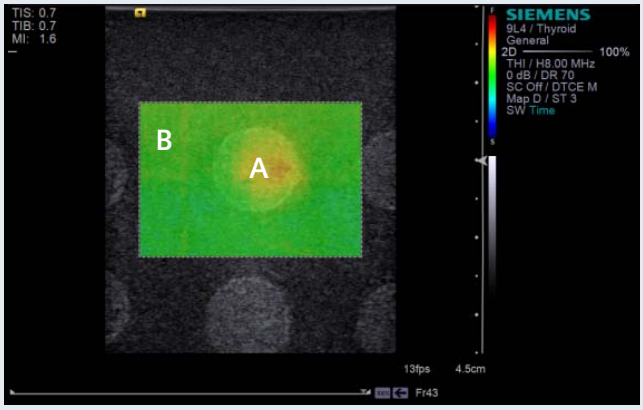

Shear Wave Travel Time

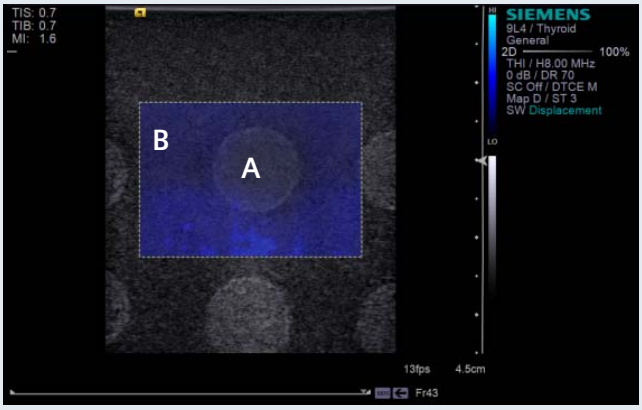

Shear Wave Displacement

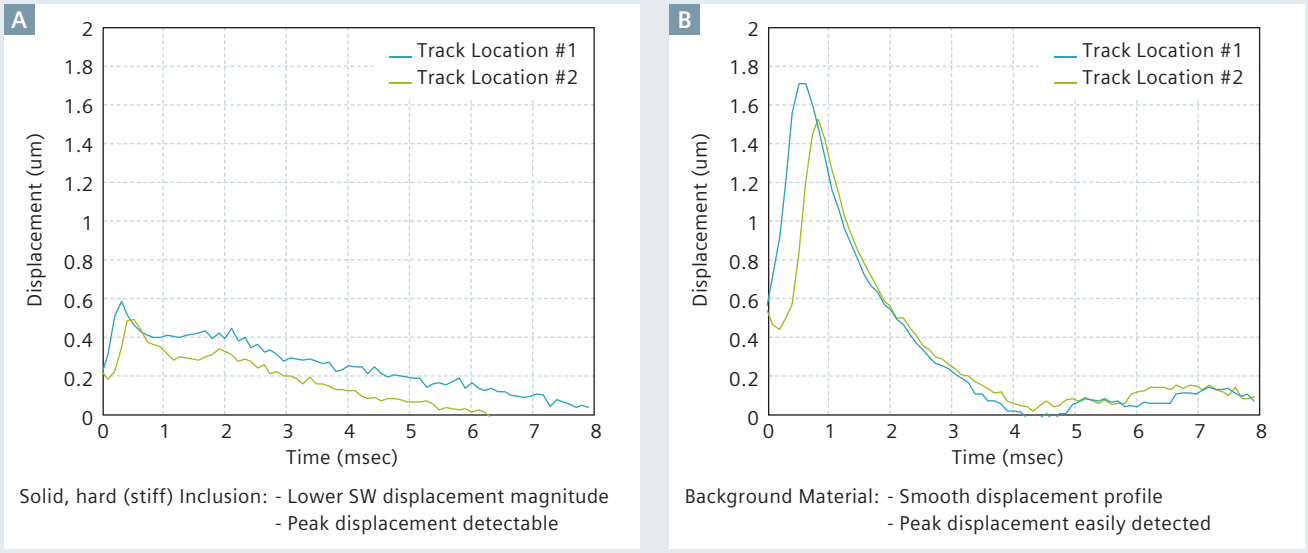

Figure 15: Tissue Mimicking Elasticity Phantom images with labeled regions: (A), a stiff solid inclusion and (B) solid elastic background material. In the lower shear wave profiles as detected with RF acoustic data from paired detection beams, the stiff inclusion area in (A) is a smooth but low displacement magnitude shear wave profile. The smooth, higher tissue displacement response of (B) indicates elastic material with the ability to detect a peak in each of the two displacement profiles at slightly different times and location, where accurate shear wave velocity can be estimated. Note the high quality shear wave signal area representing both the stiff inclusion area and elastic background material in the SW Quality display in the upper right image.

ARFI AUROC F0-2 vs F3, 4 only	Disease	N	AUROC	Optimal Vs Cutoff	Sensitivity	Specificity	PPV	NPV	Technical Adequacy Rate
Fierbinteanu-Braticevici, et al	HCV	74	0.993	1.54 m/s	97%	100%	100%	97%	100.0%
Lupsor, et al	HCV	112	0.869	1.61 m/s	97%	95%	92%	86%	91.1%
Goertz, et al	HCV, HBV	77	0.920	Not reported					96.7%
Friedrich-Rust, et al	HCV, HBV	81	0.930	1.55 m/s	82%	82%	88%	97%	100.0%
Takahashi, et al	CLD	80	0.940	1.44 m/s	96%	96%	81%	96%	100.0%
Yoneda, et al	NAFLD	64	0.973	1.77 m/s	100%	100%	71%	100%	100.0%
Palmeri, et al	NAFLD	135	0.900	N/A	90%	90%	NR	NR	88.5%
Rizzo, et al	HCV	139	0.940	1.70 m/s	91%	86%	80%	94%	100.0%

Table 1: Results of Multiple Independent Studies in the Diagnosis of Advanced Liver Fibrosis (Metavir > F2).

Imaging Method	AUROC	At Optimal Cutoff Value	
		% Sensitivity	% Specificity
Perfusion Imaging (CT)	0.791-0.824	76.9-84.6	71.4-78.5
Apparent Diffusion Coefficient (MR)	0.54-0.92 (median = 0.83)	0.52-0.88 (median = 0.73)	0.71-0.90 (median = 0.78
MR Elastography liver stiffness (MRE)	0.92-0.99 (median = 0.98)	0.78-0.97 (median = 0.92)	0.87-0.97 (median = 0.96)
Transient Elastography (TE)	0.88-0.91 (median = 0.89)	0.58-0.95 (median = 0.82)	0.78-0.97 (median = 0.90)
Virtual Touch Quantification (ARFI)	0.87-0.99 **(median = 0.94)**	0.79-1.00 **(median = 0.96)**	0.79-1.00 **(median = 0.92)**

Table 2: Comparison of the Accuracy of Different Imaging Methods for Diagnosis of Advanced Fibrosis.

Clinical Utility in Liver Imaging

New non-invasive techniques have been a research priority for the diagnosis and follow-up of chronic liver disease in recent years. The gold standard for diagnosing and monitoring the progression of liver fibrosis is a liver biopsy. Yet there are known limitations of liver biopsy that make it less than ideal for ongoing assessment of disease progression. Percutaneous biopsy underestimates or overestimates fibrosis stage or grade in up to 33% of cases [3], and is not representative of the distribution of fibrosis throughout the liver. Histologic analysis is also prone to inter-observer variability [3].

Virtual Touch quantification has been extensively studied in chronic liver disease [4–13]. These studies have examined the diagnostic accuracy of Virtual Touch in multiple etiologies, including chronic hepatitis (HBV, HCV), non-alcoholic fatty liver disease (NAFLD) and non-alcoholic steato-hepatitis (NASH). Table 1 summarizes the results of several studies conducted to determine the diagnostic accuracy of Virtual Touch quantification in advanced liver fibrosis and cirrhosis. It is important to note the high technical success rate of Virtual Touch quantification in these studies.

As reported in these studies, Virtual Touch quantification has proven to be rapid, reliable and reproducible in the measurement of shear wave velocity in the liver. Because it is a software option on some Siemens' ACUSON S Family ultrasound systems, it is easy and convenient to use in conjunction with a standard abdominal sonogram, thus it is potentially one of the most accessible non-invasive methods to assess chronic liver disease.

Virtual Touch quantification has advantages of lower utilization cost without sacrificing diagnostic accuracy compared to other imaging techniques used for the assessment of advanced liver fibrosis, as shown in Table 2.

Site	Total Lesions	Malignant Lesions	E/B-mode Ratio ≥ 1	Sensitivity	Benign Lesions	E/B-mode Ratio < 1	Specificity
1	251	54	54	100%	197	188	95.4%
2	79	40	40	100%	39	26	66.7%
3	206	90	87	96.7%	116	100	86.2%
4	52	14	14	100%	38	29	76.3%
5	34	18	18	100%	16	12	75.0%
6	13	6	6	100%	7	6	85.7%
Total	635	222	219	98.6%	413	361	87.4%

Table 3: Multi-center Study Results in the Differentiation of Malignant Breast Lesions from Benign with eSie Touch Elasticity Imaging.

Richard G. Barr MD, PhD [1, 2], Logan B. Lackey II MBA, BS [2], William E. Svensson MD [3], Corinne Balleyguier MD [4], Carmel Smith [5], Stamatia Destounis MD [6]

[1] Radiology Consultants Inc., Youngstown, OH USA,
[2] Northeastern Ohio Universities Colleges of Medicine and Pharmacy (NEOUCOM), Rootstown, OH USA,
[3] Nuclear Medicine Imaging Department, Charing Cross Hospital, Hammersmith, London W6 8RF, United Kingdom,
[4] Service de Radiodiagnostic, 94805 Villejuif Cedex, France,
[5] Queensland Imaging Center, Brisbane, Australia,
[6] Elisabeth Wende Breast Care LLC, Rochester, NY USA

Clinical Utility in Breast Imaging

Ultrasound has become a front-line imaging modality in the diagnosis of breast cancer, especially in women with dense breasts. While complementary to mammography, it provides additional information about the morphology of breast lesions. Standardization of the interpretation of breast ultrasound images has improved with the BI-RADS® scoring system and automated breast volume scanning. However, despite these recent advances, conventional ultrasound is limited in its ability to characterize lesions as malignant or benign. Therefore, breast biopsy is the standard of care for the management of patients with equivocal lesions. eSie Touch elasticity imaging has been shown to be a highly sensitive imaging method to determine the risk that a suspected lesion is malignant. A recent multi-center trial studied the ability of eSie Touch elasticity imaging to differentiate malignant from benign lesions by using the ratio of the lesion area in the elastogram to the lesion area in conventional B-mode imaging (E/B-mode ratio). An additional objective of the study was to evaluate the reproducibility of results across multiple centers. Results in Table 3 indicate the high sensitivity of eSie Touch elasticity imaging to identify cancerous lesions when the area of the lesion in the elastogram is greater than the area in B-mode.

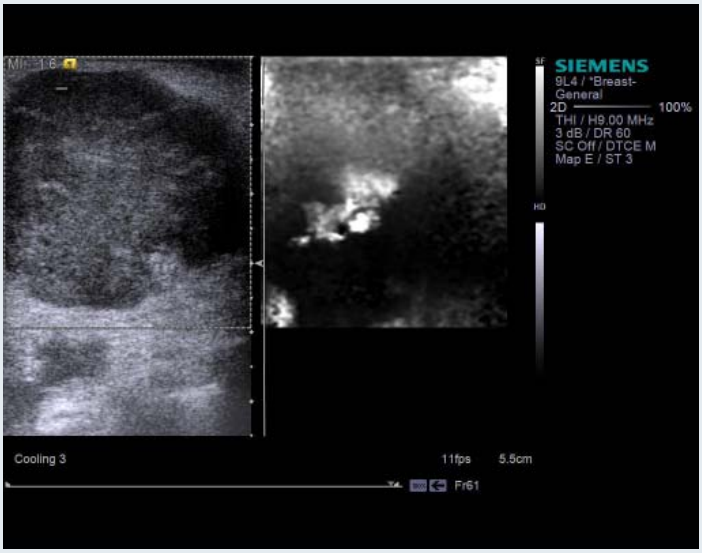

Figure 17: Complex Breast Lesion with Necrosis (arrow) Not Visible in B-mode Imaging.

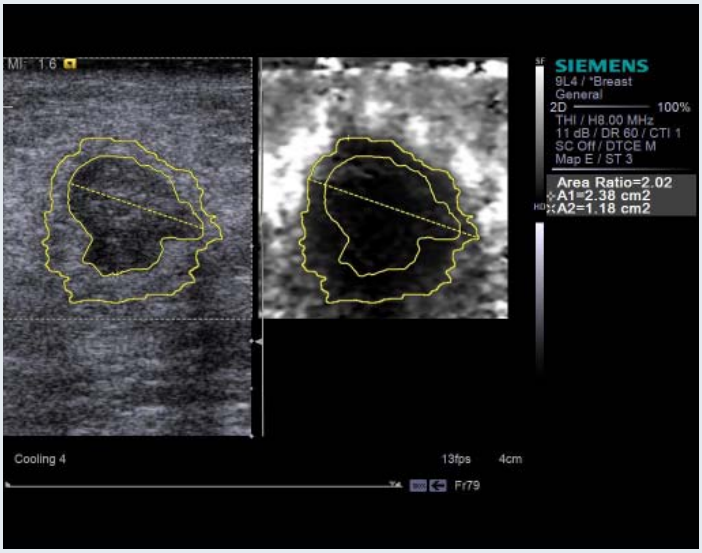

Figure 18: E/B Area Ratio (arrow) Assessment of a Breast Lesion with Virtual Touch* Imaging.

*Not commercially available in the USA.

Figure 17 is an example of a breast lesion with complex morphology. Note the ability of Virtual Touch imaging to differentiate small regions of high elasticity within the tumor. The E/B ratio of breast lesions can be assessed with Virtual Touch imaging as with eSie Touch elasticity imaging, as demonstrated in Figure 18 for area ratio. While Virtual Touch imaging has improved the resolution and reproducibility of breast elastography, it is still a qualitative image that represents relative elasticity differences of lesions compared to surrounding tissues. However, it does not indicate whether the surrounding tissue is normal.

Recently, Virtual Touch IQ has been developed to combine the qualitative and quantitative elements of Virtual Touch imaging and quantification into one image. Using more sophisticated pulse sequencing and shear wave detection algorithms, a two dimensional image of shear wave velocities now provides additional information. With the ability to accurately measure shear wave (SW) velocities from 0.5 to 10 meters per second, tissues with a wide range of elastic properties can be reliably imaged. Breast lesions in particular can span an unusually wide range of elastic values, requiring the ability to generate and track shear waves that are quickly attenuated and absorbed in very stiff tissue. The unique capabilities of Virtual Touch

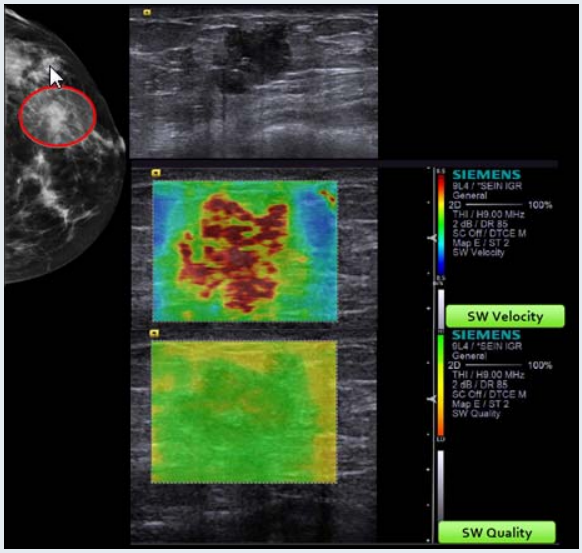

Figure 19: Virtual Touch IQ in a well visualized Intraductal Carcinoma (IDC) where the shear wave is adequately formed:
- Well visualized IDC in breast
- Uniform high SW Velocity in lesion
- SW Quality display indicates good SW velocity estimate throughout lesion

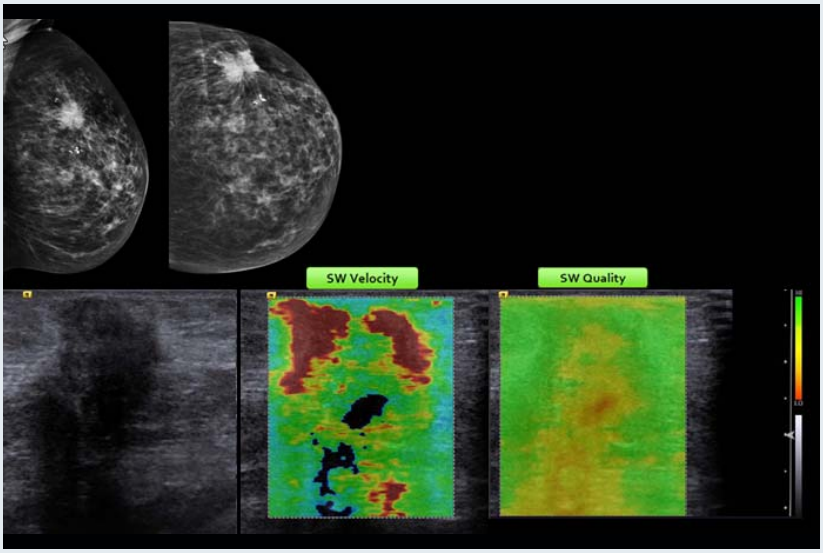

Figure 20: Virtual Touch IQ in a poorly visualized BI-RADS 5 IDC due to high attenuation in the lesion:
- Lesion is highly attenuating (Shadowing in B-mode ultrasound)
- High shear wave velocity "ring" in VTIQ
- Poor shear wave quality in center
- SW Quality display differentiates where the WS velocity estimate is accurate and where the SW velocity estimate is poor, aiding in image interpretation

IQ in these hard breast cancers are enabled by the optimal selection of transducer, frequency, pulse sequencing and tracking algorithms specifically optimized to address challenging cases.

In cases where very hard, large cancerous lesions tend to absorb and attenuate the shear wave and disrupt the ability to estimate shear wave velocity, the unique Virtual Touch IQ display modes such as SW Quality and SW Displacement may be valuable in understanding whether the shear wave was adequately formed.

This important capability allows the user to distinguish artifacts in the SW Velocity image, increasing diagnostic accuracy and diagnostic confidence. Figures 19 and 20 illustrate the clinical utility of the SW Quality display feature in two cases of breast cancer where the shear wave adequately formed (Figure 19) and where the extremely high attenuation of the tumor in both the B-mode and SW Velocity image is apparent (Figure 20). In this case, the shear wave does not adequately form in the lesion center; however, the low quality of the shear wave as indicated in the SW Quality image explains this phenomenon.

Conclusion

Tissue Strain Analytics is a promising new field for research and routine clinical application for diagnostic ultrasound. New clinical uses are found every day as this exciting new technology becomes more widely available. We have only begun to explore the potential of eSie Touch elasticity imaging and the extensive suite of Virtual Touch applications in the detection, diagnosis, treatment and follow-up of cancer, chronic liver disease, musculoskeletal degeneration and injury, as well as other diseases. The routine use of these applications is gaining international clinical acceptance, and in many institutions it has already become a new standard of care.

Siemens continues to develop and expand the diagnostic and interventional capabilities of our portfolio of Tissue Strain Analytics applications and promises to continue its leadership role in this exciting new field. Further studies are ongoing to validate the clinical utility of eSie Touch and Virtual Touch applications in new application areas of varying etiology. In liver and breast applications, studies with larger patient populations are required to confirm the preliminary results of prior studies.

References

[1] Wellman, et. al. Breast Tissue Stiffness in Compression is Correlated to Histological Diagnosis. Journal of Biomechanics. 1999.

[2] Rosen J, Brown J, De S, Sinanan M. Biomechanical Properties of Abdominal Organs In Vivo and Postmortem Under Compression Loads. Journal of Biomechanical Engineering. 2008; Vol. 130.

[3] Regev A, Berho M, Jeffers LJ, Milikowski C, Molina E, Pyrsopoulos N, Feng Z, Reddy KR, Schiff E. Sampling Error and Intraobserver Variation in Liver Biopsy in Patients With Chronic HCV Infection. American Journal of Gastroenterology. 2002; Vol. 97, No. 10.

[4] Fierbinteanu-Braticevici C, Andronescu D, Usvat R, Cretoiu D, Cristian B, et al. Acoustic Radiation Force imaging sonoelastography for noninvasive staging of liver fibrosis. World Journal of Gastroenterology. 2009; Nov 28; 15(44): 5525-5532.

[5] Goertz RS, Zopf Y, Jugl V, Heide R, Janson C, et al. Measurement of Liver Elasticity with Acoustic Radiation Force Impulse (ARFI) Technology: An Alternative Noninvasive Method for Staging Liver Fibrosis in Viral Hepatitis. Ultraschall in Med 2010; 31: 151-155.

[6] Lupsor, M, Badea R, Stefanescu H, Sparchez Z, Branda H, et al. Performance of a New Elastographic Method (ARFI technology) Compared to Unidimensional Transient Elastography in the Noninvasive Assessment of Chronic Hepatitis C. Preliminary Results. Journal of Gastrointestinal Liver Disease. 2009; Sep;18 (3): 303-310.

[7] Friedrich-Rust M, Wunder K, Kriener S, Sotoudeh F, et al. Liver Fibrosis in Viral Hepatitis: Noninvasive Assessment with Acoustic Radiation Force Impulse Imaging versus Transient Elastography. Radiology. 2009; 252(2): 595-604.

[8] Takahashi H, Ono N, Eguchi Y, Eguchi T, Kitajima Y, et al. Evaluation of acoustic radiation force impulse elastography for fibrosis staging of chronic liver disease: a pilot study. Liver International. 2009; ISSN 1478-3223: 538-545.

[9] Iijima H, Tanaka H, Yoshida M, Ikeda N, Yamamoto T, et al. Noninvasive diagnosis of Liver Fibrosis using Virtual Touch Tissue Quantification. Hepatology. 2009; Oct; 50(40: Volume 50, Number 4. 54-55.

[10] Boursier J, Isselin G, Fouchard-Hubert I, Oberti F, Dib N, et al. Acoustic radiation force impulse: a new ultrasonographic technology for the widespread noninvasive diagnosis of liver fibrosis. Eur J Gastroenterol Hepatol. 2010; Apr 30.

[11] Yoneda M, Suzuki J, Kato S, Fujita K, Nozaki Y, Hosono K, Saito S, Nakajima A. Non-Alcoholic Fatty Liver Disease: US-Based Acoustic Radiation Force Impulse Elastography. Radiology. 2010; 256(2): 640-647.

[12] Rizzo L, Calvaruso V, Cacapardo B, Alessi N, Attanasio M, Petta S, Fatuzzo F, Montineri A, Mazzola A, L'abbate L, Nunnari G, Bronte F, Di Marco V, Craxi A, Camma C. Comparison of Transient Elastography and Acoustic Radiation Force Impulse for Non-Invasive Staging of Liver Fibrosis in Patients with Chronic Hepatitis C. Am J Gastroenterol advance online publication. 4 October 2011; doi: 10.1038/ajg.2011.341.

[13] Palmeri M, Wang M, Rouze N, Abdelmalek M, Guy C, Moser B, Diehl A, Nightingale K. Noninvasive evaluation of hepatic fibrosis using acoustic radiation force-based shear stiffness in patients with nonalcoholic fatty liver disease. Journal of Hepatology. 2011; Vol. 55, 666–672.

Standalone clinical images may have been cropped to better visualize pathology.

Global Siemens Headquarters
Siemens AG
Wittelsbacherplatz 2
80333 Muenchen
Germany

Global Siemens Healthcare Headquarters
Siemens AG
Healthcare Sector
Henkestrasse 127
91052 Erlangen
Germany
Phone: +49 9131 84-0
www.siemens.com/healthcare

Legal Manufacturer
Siemens Medical Solutions USA, Inc.
Ultrasound
685 E. Middlefield Road
Mountain View, CA 94043 USA
Phone: 1-888-826-9702
www.siemens.com/ultrasound

Order No. A91US-224-1C-4A00 | Printed in Germany | CC 661 1212x. |

www.siemens.com/healthcare